Duct cells in development, regeneration, and transplantation: charting a path to new islets

Balak, J.R.A.

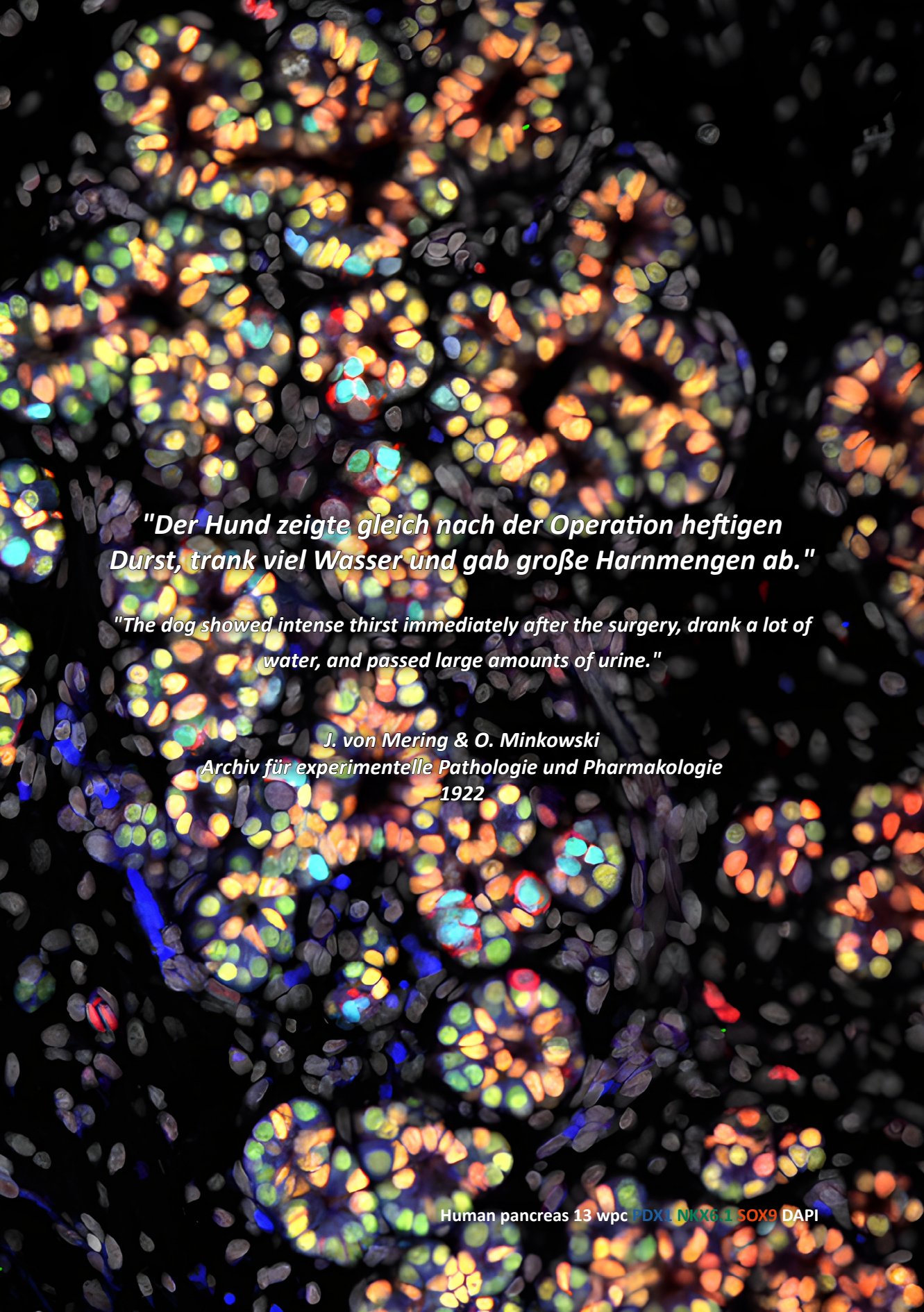
"Der Hund zeigte gleich nach der Operation heftigen Durst, trank viel Wasser und gab große Harnmengen ab."
"The dog showed intense thirst immediately after the surgery, drank a lot of water, and passed large amounts of urine."
J. von Mering & O. Minkowski
Archiv für experimentelle Pathologie und Pharmakologie
1922
Human pancreas 13 wpc PDX1 NKX6.1 SOX9 DAPI

CHAPTER| 4

Expansion of Adult Human Pancreatic Tissue Yields Organoids Harboring Progenitor Cells With Endocrine Differentiation Potential

Cindy J.M. Loomans[1,2,*], Nerys Williams Giuliani[1,2,*], Jeetindra R.A. Balak[2], Femke Ringnalda[1], Léon van Gurp[1], Meritxell Huch[1,3], Sylvia F. Boj[1], Toshiro Sato[4], Lennart Kester[1], Susana M. Chuva de Sousa Lopes[5], Matthias S. Roost[5], Susan Bonner-Weir[6], Marten A. Engelse[2], Ton J. Rabelink[2], Harry Heimberg[7], Robert G.J. Vries[1], Alexander van Oudenaarden[1], Françoise Carlotti[2], Hans Clevers[1], Eelco J.P. de Koning[1,2]

[1]Hubrecht Institute/KNAW and University Medical Center Utrecht, Utrecht, the Netherlands
[2]Dept of Internal Medicine, Leiden University Medical Center, Leiden, the Netherlands
[3]Wellcome Trust/Cancer Research UK, Cambridge, the United Kingdom
[4]Dept of Gastroenterology, Keio University, Tokyo, Japan
[5]Dept of Anatomy and Embryology, Leiden University Medical Center, Leiden, the Netherlands
[6]Islet Cell & Regenerative Biology, Joslin Diabetes Center, Boston, USA
[7]Beta Cell Neogenesis, Vrije Universiteit Brussel, Brussels, Belgium

Stem Cell Reports. 2018 Mar 13;10(3):712-724

Summary

Generating an unlimited source of human insulin-producing cells is a prerequisite to advance beta cell replacement therapy for diabetes. Here, we describe a 3D culture system that supports the expansion of adult human pancreatic tissue and the generation of a cell subpopulation with progenitor characteristics. These cells display high aldehyde dehydrogenase activity ($ALDH^{hi}$), express pancreatic progenitor markers (PDX1, PTF1A, CPA1, and MYC), and can form new organoids in contrast to $ALDH^{lo}$ cells. Interestingly, gene expression profiling revealed that $ALDH^{hi}$ cells are closer to human fetal pancreatic tissue compared with adult pancreatic tissue. Endocrine lineage markers were detected upon *in vitro* differentiation. Engrafted organoids differentiated toward insulin-positive (INS^{+}) cells, and circulating human C-peptide was detected upon glucose challenge 1 month after transplantation. Engrafted $ALDH^{hi}$ cells formed INS^{+} cells. We conclude that adult human pancreatic tissue has potential for expansion into 3D structures harboring progenitor cells with endocrine differentiation potential.

Highlights

- A 3D culture system can support the expansion of adult human pancreatic tissue
- An $ALDH^{hi}$ cell subpopulation is identified in these organoids
- $ALDH^{hi}$ cells, and not $ALDH^{lo}$ cells, are capable of forming new organoids
- $ALDH^{hi}$ cells show endocrine differentiation potential

In the context of beta cell replacement therapy for diabetes, de Koning and colleagues describe a 3D culture platform that supports *ex vivo* expansion of human pancreatic tissue as organoids. These organoids harbor a subpopulation of $ALDH^{hi}$ cells that display proliferative capacity and can differentiate to an endocrine fate.

Introduction

Beta cell replacement therapy is an attractive therapy to achieve normoglycemia in patients with diabetes mellitus due to severe beta cell failure[1,2]. The shortage of organ donors severely limits the number of patients that are eligible for current beta cell replacement therapy, *i.e.*, pancreas or islet transplantation. Mature human beta cells cannot be expanded *in vitro* without complex dedifferentiation and redifferentiation processes[3,4]. Thus, there is an unmet clinical need to generate insulin-producing cells from alternative cell sources to make this therapy more widely available.

Several types of cells have been studied as possible sources of insulin-producing cells, including human embryonic stem cells (hESCs) and human induced pluripotent stem cells (iPSCs). While the phenotype of these cells has long been characterised by immature maturation[5], recently more glucose-responsive cells have been generated from human pluripotent stem cells *in vitro*[6,7], but safety remains a major concern for any regenerative strategy using hESCs or iPSCs[8,9]. An attractive alternative could be the use of putative progenitor cells from adult human pancreas that give rise to

the endocrine lineage. Histological studies of human pancreas indicate that neogenesis of insulin-producing cells is associated with the ductal tree in obesity and pregnancy[10,11]. Other studies have also shown that some insulin-producing cells can be generated from cultured human pancreatic ductal tissue[12-15]. We recently showed that *in silico* analysis of single-cell transcriptome profiles of human adult pancreatic cells using a StemID algorithm predicts a distinct subpopulation of ductal cells with multipotential differentiation potential[16]. In mice, the existence of postnatal endocrine progenitors within the pancreatic ductal population has become controversial, with lineage-tracing experiments showing contradictory results. Although several studies were able to detect endocrine cells derived from the ductal lineage postnatally or after injury[17-20], others did not find this[21-23].

At present, expansion of human pancreatic cells in a standard, 2D culture system is hampered by the transition of both islet[4,24] and duct cells[25-27] to a mesenchymal cell-like phenotype during passaging. This approach does not provide the natural 3D environment of tissues, and thus important information of cell orientation and polarity for proliferation, growth, and differentiation are lost. In fact, proper alignment and polarization of progenitor cells is known to be required for successful differentiation of fetal pancreatic progenitor cells[28,29], and 3D culture of fetal murine pancreatic progenitors can be used to unravel and mimic niches important in pancreas development[30]. Thus, it is tempting to hypothesize that 3D culture of adult human pancreatic tissue may provide a microenvironment that enhances expansion and differentiation of pancreatic progenitors.

A Matrigel-based 3D culture system was developed in our institute that yields organoids from stem cells in different organs, with the capacity for long-term expansion and generation of functional differentiated organ-specific cells[31-33]. Single isolated adult mouse pancreatic progenitor cells can be expanded by forming colonies or organoids in a Matrigel-based system[30,32,34]. We observed that these progenitor cells are derived from the ductal tree, express the stem cell marker leucine-rich repeat containing G protein-coupled receptor 5 (Lgr5) in culture and are able to differentiate toward the endocrine lineage[32].

Results

Human pancreatic tissue expands as budding organoids

Islet-depleted pancreatic tissue after collagenase digestion was obtained from 35 non-diabetic organ donors (age 53.6 ± 12.1 years and BMI 24.7 ± 4.0 kg/m^2) and one organ donor with a history of type 1 diabetes (age 48 years, BMI 21 kg/m^2). After mechanical dissociation the small clumps of tissue were embedded in Matrigel and supplied with an epidermal growth factor/Noggin/R-spondin-based expansion medium. More than 90% of small pancreatic cell clusters formed budding structures within 3 days (**Movie S1**), and expanded with a cauliflower-like appearance by day 7 (**Figure 1A**). Some larger cyst-like structures were present in the organoids (**Figure 1A**). Organoids could be passaged without macroscopic changes in phenotype (**Figure 1B**), and maintained in culture for at least 10 passages (**Figure 1C**). The calculated rate for cell doubling was approximately 67 hr during passage 0 (P0) (n = 3). Growth rate slightly diminished upon passaging (**Figure 1C**). The

proportion of small budding structures and cyst-like structures varied among donors (**Figure S1A**). Organoids could also be generated from pancreatic tissue from an organ donor with a history of type 1 diabetes (**Figure S1B**).

Next, we analysed the cellular composition of organoids in the expansion phase. At day 7 (P0), 92.3% ± 5.4% of organoid cells were positive for the epithelial marker keratin 19 (KRT19), indicating a ductal phenotype (**Figure 1D and 1E**). Also at passage 3 (P3), the vast majority of the cells still had a ductal phenotype (87.2% ± 8.4% of organoid cells were $KRT19^+$). No insulin-positive (INS^+), glucagon-positive (GCG^+), or amylase-positive (AMY^+) cells were detected in the organoids at day 7 of the expansion phase (P0) (**Figure 1D and 1E**). The organoids were organised as $KRT19^+$ cells lining cystic or smaller elongated luminal spaces (**Figure 1E**). In both early and late passages, cells appeared polarized with positive mucin-1 (MUC1) staining at the luminal side of the $KRT19^+$ epithelial lining (**Figure 1E**). Although human pancreatic cells in 2D culture systems acquire a mesenchymal cell-like phenotype[4,25-27,35], few vimentin-positive cells (<2%) were observed in our organoid cultures at P0 or P3 (**Figure 1E**). Thus, small adult human pancreatic cell clusters can be expanded and passaged in 3D culture, generating polarized ductal budding structures.

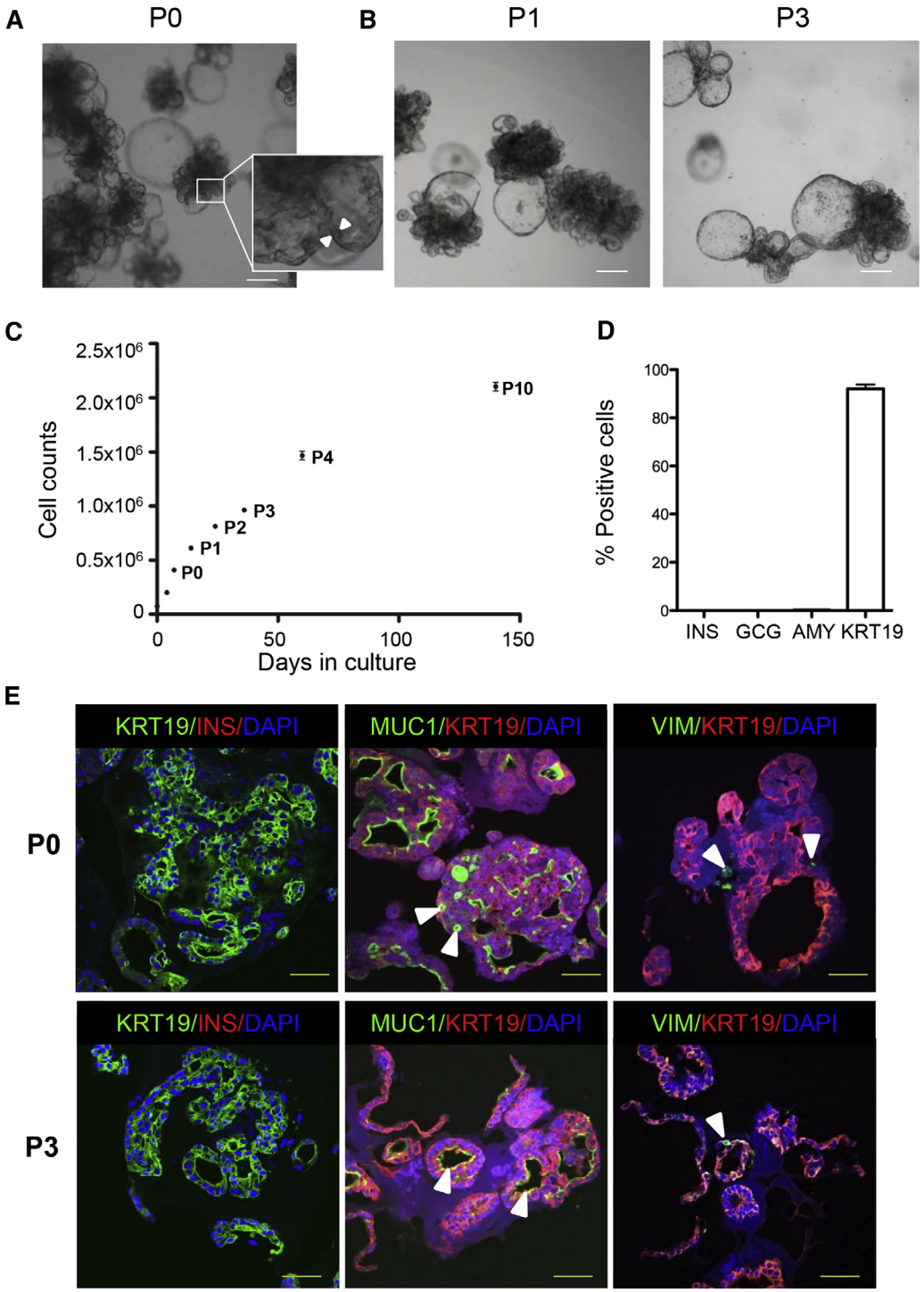
A
P0
B
P1
P3
C
Cell counts
2.5x10^6
2.0x10^6
1.5x10^6
1.0x10^6
0.5x10^6
0
P0
P1
P2
P3
P4
P10
0
50
100
150
Days in culture
D
% Positive cells
100
80
60
40
20
0
INS
GCG
AMY
KRT19
E
P0
P3
KRT19/INS/DAPI
MUC1/KRT19/DAPI
VIM/KRT19/DAPI

Figure 1. Characterization of human pancreatic organoids during expansion in a 3D Culture system

(**a**) Bright-field image of pancreatic organoids (P0), expanded for 7 days in a 3D Matrigel-based culture system, reveals extensive growth with multiple budding structures. Some larger buds have a cyst-like appearance. The insert shows a close-up image of the cell lining (between arrowheads) in a budding structure. Scale bar, 100 µm. (**b**) Passaged organoids (P1 and P3 are shown) expanded in similar conditions as P0 (A), also forming budding structures in a cauliflower-like configuration. Scale bar, 100 µm. (**c**) Growth curve of pancreatic organoids cultured for 140 days. Cell numbers were counted on days 0, 4, and 7 (P0), and at the end of subsequent passages. Cells in five wells per time point were counted (mean ± SEM). The expansion curve is representative of n = 3 donors. (**d**) Quantification of number of cells positive for INS, GCG, AMY, or KRT19 by immunohistochemistry in organoids on day 7 of expansion culture (n = 8 donors; at least 10 organoids/donor were counted; mean ± SEM). DAPI was used as nuclear counterstain. (**e**) Non-passaged organoids (P0, upper panels) have similar features compared with passaged organoids (P3, lower panels). Left panels: the majority of the cells are KRT19$^+$ (green), with no INS$^+$ cells (red) detected during the expansion phase. Middle panels: MUC1 (green) staining at the apical cell border indicates polarization of the duct cells. Small lumena are visible within the organoids (arrowheads). Right panels: few vimentin-positive (VIM$^+$) cells (green) are present in the organoids (arrowheads). n = 5 donors; >15 organoids/donor were stained. DAPI was used as nuclear counterstain. Scale bars, 50 µm. See also **Figure S1**.

Human pancreatic organoids display pancreatic progenitors clustered toward the tips of the budding structures

Since extensive growth by budding was observed, we determined the proliferative capacity of the budding structures. Quantification showed that 27.3% ± 8.7% of the cells within an organoid were Ki67$^+$ at day 7 of expansion (**Figure 2A**). Only a few Ki67$^+$ cells were negative for the duct marker KRT19 (1.3% ± 0.8% of Ki67$^+$ cells). Ki67$^+$ cells were mainly observed in tips of buds and were not frequently observed in trunk regions (**Figure 2B**). Also, budding structures with wide tips and narrow trunks were present in the organoids (**Figure 2B and 2C**). Labelling with the nucleoside analog 5-ethynyl-2'-deoxyuridine that incorporates into newly synthesized DNA further confirmed the location of the proliferative cells toward the tip region (data not shown).

Based on the configuration of the budding structures, we hypothesized that the tips of the budding structures would be enriched for pancreatic progenitor cells, as has been reported for mouse fetal pancreatic development[36,37]. Immunostaining of the organoids for the pancreatic progenitor markers *pancreatic and duodenal homeobox 1* (PDX1) and *SRY (sex-determining region Y) box 9* (SOX9) (**Figure 2B**) showed high PDX1 expression in the budding structures of the organoids, particularly in tip regions, while SOX9 was more homogeneously distributed (**Figure 2B**). SOX9 and PDX1 gene expression increased during expansion (**Figure S2A**). Furthermore, gene expression of LGR5 increased during this time (**Figure S2B**), and a subset of cells in budding structures clearly expressed LGR5 mRNA, as assessed by smFISH (**Figure S2C**). No *neurogenin-3*-positive (NEUROG3$^+$) cells were observed in organoids in the expansion phase (**Figure 2A**). Next, we exposed the organoids to a fluorescent reagent (Aldefluor) that identifies progenitor cells based on their increased aldehyde dehydrogenase (ALDH) activity. Pancreatic progenitors with high

expression of ALDH1 isoforms have recently been identified in both developing and adult mouse pancreas[38,39]. Cells concentrated in the tips of the budding structures showed high ALDH activity (**Figure 2C**). The Aldefluor reagent is optimised to detect enzyme activity of ALDH1 isoforms, and we found that ALDH1A1 immunostaining co-localized with both KRT19^{+} and KRT19^{-} cells in the tips of the organoid buds, indicating the presence of heterogeneous populations of ALDH1A1^{+} cells (data not shown). High ALDH activity arose during organoid culture as no ALDH^{hi} cells were found in the d0 islet-depleted tissue (n = 3; data not shown). LGR5 gene expression was higher in sorted ALDH^{hi} compared with ALDH^{lo} cells (**Figure S2D**).

Single ALDH^{hi} cells show progenitor characteristics

To determine whether ALDH^{hi} cells have characteristics of progenitor cells, organoids were dispersed into single cells, labelled with Aldefluor, and sorted by fluorescence-activated cell sorting (FACS) (ALDH^{lo} cells 34.0% ± 7.4% and ALDH^{hi} cells 25.4% ± 6.0%, n = 5) (**Figure 2D**). A subpopulation of ALDH^{hi} cells derived from organoids was able to generate small cyst-like colonies in 3D culture (2.2% ± 0.8% of ALDH^{hi} cells), in marked contrast to ALDH^{lo} cells that formed no colonies (**Figure 2E, 2F, and S3A**). When organoids derived from single-sorted ALDH^{hi} cells were immunostained for ALDH1A1, both ALDH1A1^{+} and ALDH1A1^{-} cells were observed, indicating the generation of a heterogeneous cell population from a single ALDH^{hi} cell (**Figure S3B**). When these labelled organoids were sorted once more, yet again only ALDH^{hi} cells showed colony-forming potential in 3D culture (data not shown). Interestingly, complex budding structures were not observed when single ALDH^{hi} cells were expanded, which could indicate the requirement of supporting cells for self-assembly into a ductal-tree-like configuration (**Figure S3A**).

Next, we characterised the ALDH^{hi} cell population for the presence of markers previously described for multipotent progenitor cells in mouse pancreatic organogenesis[36]. Gene expression levels of the markers carboxypeptidase A1 (CPA1) and pancreas-specific transcription factor, 1a (PTF1A) were significantly upregulated in ALDH^{hi} cells compared with the ALDH^{lo} fraction (**Figure 2G**). Immunoreactivity for CPA1 was found in ALDH1A1^{+} cells in the tips of organoid budding regions, but some ALDH1A1^{+} cells were CPA1^{-} (**Figure 2H**). Importantly, these ALDH1A1^{+} cells were negative for the acinar cell marker amylase (**Figure S3C**). Many ALDH1A1^{+} cells in the tips of budding regions buds also co-stained for PDX1 (**Figure S3D**). Genes that are known to be upregulated in mouse centroacinar (CAC) cells, such as HES1, SOX9, SCA1, MET, NES, and HEY1[39,40], were analysed in sorted ALDH^{hi} and ALDH^{lo} cells. No upregulation of these markers was present in ALDH^{hi} compared with ALDH^{lo} cells (**Figure S3E**). HES1^{+} cells were present in expanded organoids after 7 days, but their distribution was not well defined (**Figure S3F**). Thus, a subpopulation of ALDH^{hi} cells within human pancreatic organoids has colony formation capacity and expresses pancreatic progenitor markers.

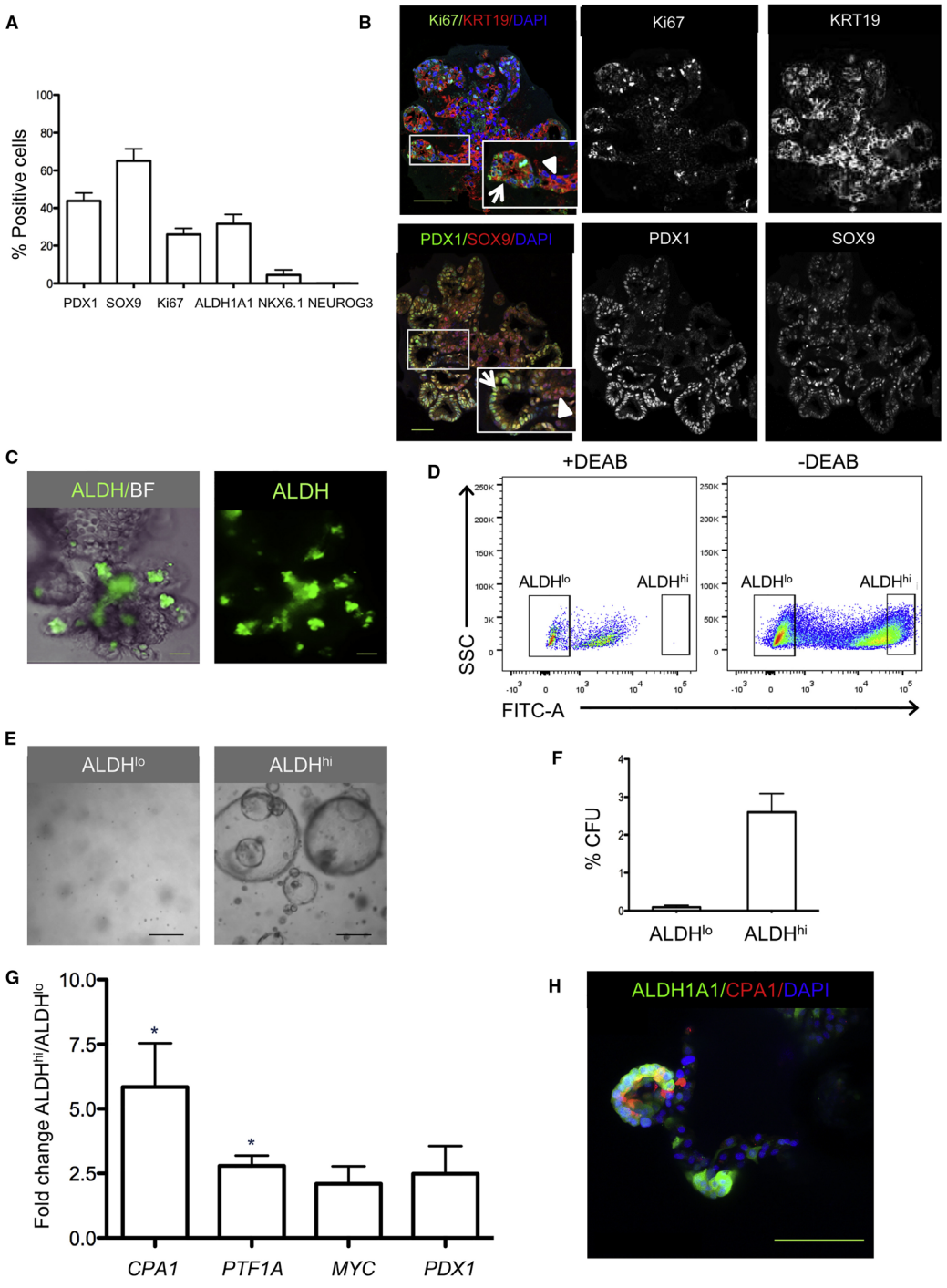
A
% Positive cells
100
80
60
40
20
0
PDX1 SOX9 Ki67 ALDH1A1 NKX6.1 NEUROG3
B
Ki67/KRT19/DAPI
Ki67
KRT19
PDX1/SOX9/DAPI
PDX1
SOX9
C
ALDH/BF
ALDH
D
+DEAB
-DEAB
ALDHlo
ALDHhi
SSC
FITC-A
E
ALDHlo
ALDHhi
F
% CFU
ALDHlo
ALDHhi
G
Fold change ALDHhi/ALDHlo
10.0
7.5
5.0
2.5
0.0
CPA1
PTF1A
MYC
PDX1
H
ALDH1A1/CPA1/DAPI

Figure 2. Tips of budding structures of pancreatic organoids contain cells with progenitor cell characteristics

(**a**) Quantification of cells positive for pancreatic progenitor and proliferation markers in organoids on day 7 of expansion culture. Organoids derived from four to six donors were analysed (at least ten organoids/donor). Data are expressed as mean ± SEM. (**b**) Confocal image of pancreatic organoids on day 7 of expansion. Top: organoids were stained for the proliferation marker Ki67 (green) and ductal marker KRT19 (red). Organoid budding structures show a narrow trunk region (arrowhead) and a wider tip region (arrow). Bottom: organoids were stained for SOX9 (red) and PDX1 (green). $SOX9^+$ cells were present both in the buds and in the trunk region of the organoids (arrowhead). $PDX1^+$ cells (green), which frequently co-expressed SOX9 (yellow), were mainly located in the budding structures with strong staining for PDX1 often observed in cells at the outermost tip regions (arrow). Both overlay and individual channels are depicted. DAPI was used as nuclear counterstain. Scale bars, 100 µm. (**c**) Organoids in expansion phase for 7 days were labelled with the Aldefluor fluorescent reagent system, marking progenitor cells characterised by high ALDH activity. Most $ALDH^{hi}$ cells (green) were located in the tips of organoid buds. Scale bar, 50 µm. (**d**) FACS analysis of dispersed organoid cells (after 7 days in expansion culture) labelled with Aldefluor with and without the ALDH inhibitor DEAB. The FACS plot shows how $ALDH^{hi}$ cells (***i.e.***, cells that express high ALDH activity) and $ALDH^{lo}$ cells (***i.e.***, cells that express low ALDH activity) are selected. Representative plot from n = 10 donors. (**e**) Bright-field images of sorted and expanded single $ALDH^{lo}$ cells (left panel) and $ALDH^{hi}$ cells (right panel) in Matrigel for 14 days. Scale bar, 100 µm. (**f**) Proportion of sorted $ALDH^{lo}$ and $ALDH^{hi}$ cells with colony-forming (organoid-forming) potential. Data represent mean ± SEM (n = 3 donors). (**g**) Gene expression of CPA1, PTF1A, MYC, and PDX1 in sorted $ALDH^{lo}$ and $ALDH^{hi}$ cells derived from organoids expanded for 7 days. The graph shows the gene expression ratio in $ALDH^{hi}$ to $ALDH^{lo}$ cells for the different markers. Mean ± SEM (n = 3 donors) $*P < 0.05$. (**h**) Whole-mount immunostaining for ALDH1A1 and CPA1 of organoids expanded for 7 days. Confocal images show $ALDH1A1^+$ cells (green) and $CPA1^+$ cells (red) in the tip of the budding structures. Some cells co-express the two markers. Scale bar, 50 µm. CFU, colony-forming unit. See also **Figures S2** and **S3**.

Transcriptional profiling shows clustering of $ALDH^{hi}$ cells from adult and fetal pancreatic organoids

Since the self-assembly of adult human pancreatic tissue into organoids in our 3D culture system resembles budding structures previously described in pancreatic development, we compared characteristics of organoids derived from adult pancreatic tissue (adult pancreatic organoids) with human fetal pancreatic tissue and organoids derived from this fetal pancreatic tissue (fetal pancreatic organoids). We observed that fetal pancreatic organoids displayed a similar morphology to adult pancreatic organoids under the same culture conditions (**Figure 3A**). $ALDH^{hi}$ cells were predominantly located in budding structures (**Figure 3A**). This observation strengthened our hypothesis that $ALDH^{hi}$ cells that are concentrated in tip regions have pancreatic progenitor characteristics. We set out to determine the level of similarity of these putative $ALDH^{hi}$ progenitors isolated from adult pancreatic organoids with $ALDH^{hi}$ cells derived from fetal pancreatic organoids. Global gene expression analysis revealed that $ALDH^{hi}$ cells from adult pancreatic organoids are transcriptionally closer to $ALDH^{hi}$ cells isolated from fetal pancreatic organoids than to the adult exocrine tissue they originated from (**Figure 3B and 3C**). In contrast, $ALDH^{hi}$ cells from fetal pancreatic organoids retained their more primitive identity, clustering closely to fetal pancreatic

tissue (**Figure 3B**). Furthermore, expression levels of the multipotent progenitor markers CPA1, PTF1A, PDX1, and MYC in ALDH^{hi} cells from adult pancreatic organoids were comparable with those in ALDH^{hi} cells from organoids derived from fetal pancreas (no significant difference, $p < 0.05$; data not shown).

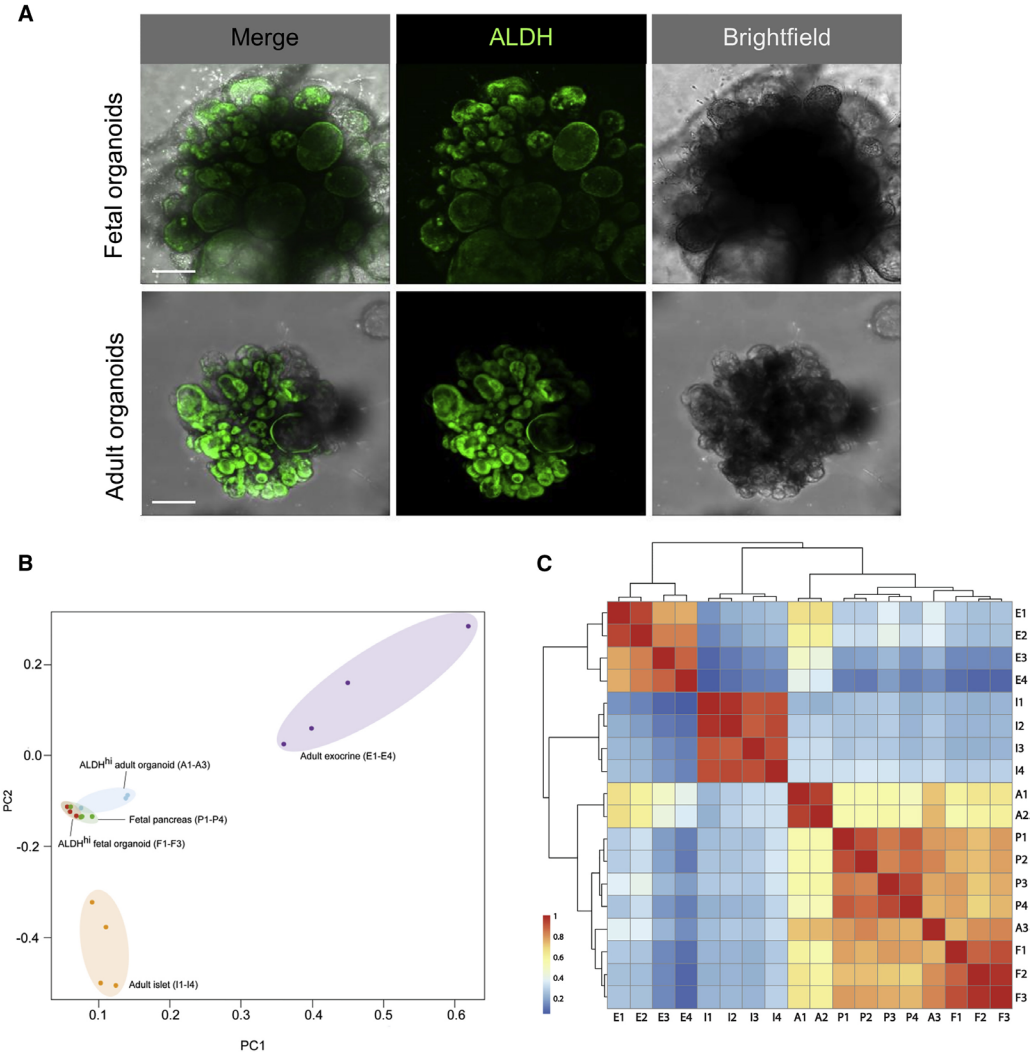

Figure 3. Transcriptional profiling shows clustering of ALDH^{hi} cells from adult and fetal pancreatic organoids

(**a**) Aldefluor labelling of adult and fetal human pancreatic organoids expanded for 7 days. Maximum projection (confocal imaging). Scale bar, 100 µm. (**b**) Principal-component analysis for gene expression profiles of the following samples: A1-A3: ALDH^{hi} cells sorted from organoids after 7 days expansion derived from human adult pancreatic tissue (age 50.0 ± 18.7 years, BMI 22.0 ± 4.0 kg/m2). F1-F3: ALDH^{hi} cells sorted from organoids after 7 days expansion derived from human fetal pancreatic tissue (gestational age: F1 9 weeks, F2 20 weeks, and F3 22 weeks). P1-P4: primary fetal pancreatic tissue (gestational age: P1 9 weeks, P2 18 weeks, P3 14 weeks, and P4 10 weeks). I1-I4: adult human islets (age 34.5 ± 17.3 years, BMI 23.8 ± 4.5 kg/m^2). E1-E4: adult exocrine (islet-

depleted) pancreatic tissue (age 63.5 ± 5.7 years, BMI 25.5 ± 3.7 kg/m^2). (**c**) Correlation cluster analysis for the gene expression profiles of the samples described in (B).

Pancreatic organoids can differentiate toward an endocrine fate *in vitro*

Since pancreatic organoids expanded from adult human exocrine tissue express progenitor markers during expansion, their differentiation potential was studied using culture conditions reported to differentiate human duct cells[13,41]. When P0 organoids were transferred to low attachment plates containing differentiation medium, their budding structure appeared to collapse and a rounded shape was seen after 7 days (**Figure 4A**). By then, growth had almost completely stopped as indicated by the near absence of Ki67$^+$ cells (0.9% ± 0.4% of total cells; **Figure 4B and 4H**) and reduced Cyclin D1 (CCND1) gene expression (**Figure 4G**). Furthermore, the proportion of ALDH1A1$^+$ cells decreased considerably from 27.0% ± 14.5% (P0 expansion day 7) to 1.4% ± 1.3% of total cells (differentiation day 7) (**Figure 4H**).

A marked increase in insulin gene expression after 7 days of differentiation was observed when compared with the end of the expansion phase (**Figure 4G**). Despite the considerable increase in insulin gene expression with differentiation, few INS$^+$ cells were observed by immunostaining (0.52% ± 0.22%; **Figure 4C and 4H**). GCG gene expression was only slightly increased between expansion and differentiation (**Figure 4G**), and no GCG$^+$ cells were present in the differentiation phase (**Figure 4H**). To exclude the possibility that insulin was taken up from the medium, we confirmed that INS$^+$ cells were also positive for human C-peptide (**Figure S4A**). No AMY$^+$ cells were observed and the majority of cells remained KRT19$^+$ during differentiation (83.4% ± 14.5% of cells; **Figure 4H**), even though gene expression of KRT19 decreased (**Figure 4G**).

Gene expression of the endocrine progenitor marker NEUROG3 and beta cell marker NKX6 homeobox 1 (NKX6.1) were significantly upregulated during the differentiation phase (**Figure 4G**). NEUROG3$^+$ cells could also be identified by immunostaining in the 'collapsed' organoids (**Figure 4E and 4H**). In addition, more cells expressed NKX6.1 in the differentiation phase compared with the expansion phase (**Figure 4F and 4H**). Conversely, no change was found in gene expression of the pancreatic progenitor markers PDX1 and SOX9 upon differentiation (**Figure 4G**) or the number of PDX1$^+$ and SOX9$^+$ cells (**Figure 4D and 4H**). Thus, upon *in vitro* differentiation, pancreatic progenitors can be directed along the endocrine lineage.

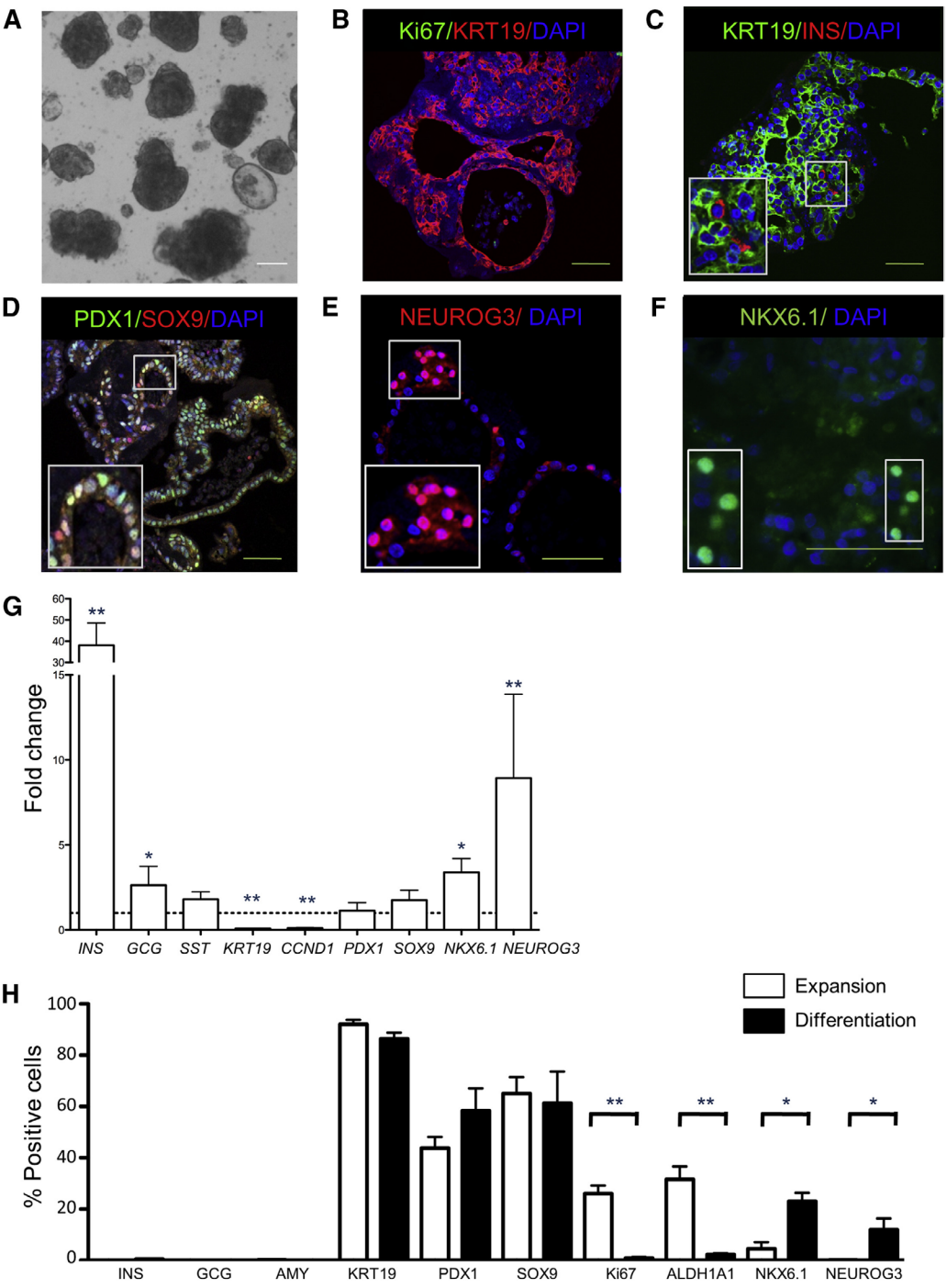
A
B
Ki67/KRT19/DAPI
C
KRT19/INS/DAPI
D
PDX1/SOX9/DAPI
E
NEUROG3/ DAPI
F
NKX6.1/ DAPI
G
Fold change
INS
GCG
SST
KRT19
CCND1
PDX1
SOX9
NKX6.1
NEUROG3
H
% Positive cells
Expansion
Differentiation
INS
GCG
AMY
KRT19
PDX1
SOX9
Ki67
ALDH1A1
NKX6.1
NEUROG3

Figure 4. Endocrine cell markers in pancreatic organoids after 7 days of *in vitro* differentiation
(**a**) Bright-field image of human pancreatic organoids initially expanded for 7 days followed by differentiation culture for 7 days. DAPI was used as nuclear counterstain. Scale bar, 100 µm. (**b**) Confocal image of pancreatic organoids immunostained for Ki67 (green) and KRT19 (red). The majority of cells were KRT19$^+$. No cells were Ki67$^+$. DAPI was used as nuclear counterstain. Scale bar, 50 µm. (**c**) Confocal image of pancreatic organoids immunostained for KRT19 (green) and INS (red). Few INS$^+$ (0.52%) cells were present. DAPI was used as nuclear counterstain. Scale bar, 50 µm. (**d**) Confocal image of pancreatic progenitor markers PDX1 (green) and SOX9 (red). DAPI was used as nuclear counterstain. Scale bar, 50 µm. (**e**) Confocal image of pancreatic progenitor marker NEUROG3 (red). DAPI was used as nuclear counterstain. Scale bar, 50 µm. (**f**) Confocal image of pancreatic progenitor marker NKX6.1 (green). DAPI was used as nuclear counterstain. Scale bar, 50 µm. (**g**) Gene expression of several markers in organoids on day 7 of differentiation compared with organoids on day 7 of expansion. Gene expression in expansion organoids were set to 1 (dotted line). Mean ± SEM, n = 8 donors. *$P < 0.05$ and **$P < 0.01$. (**h**) Percentage of cells immunostained for different markers on day 7 of expansion (white bars) compared with day 7 of differentiation (black bars) using confocal images. More than 10 organoids per donor were assessed. Mean ± SEM, n = 4-6 donors. *$P < 0.05$ and **$P < 0.01$. See also Figure S4.

Human pancreatic tissue can be cryopreserved without losing expansion or differentiation capacities

With therapeutic purposes in mind, we explored the possibility of cryopreserving pancreatic tissue before organoid expansion. Freshly retrieved tissue (day 0) was compared with cryopreserved tissue (day 0) from the same donors (n = 4). Growth of organoids with budding structures was observed from both groups (**Figure S4B**), but the organoids grown from cryopreserved starting material had more cystic appearance than organoids grown from freshly isolated material. When subjected to *in vitro* differentiation, no significant differences in gene expression were found (**Figure S4C**). Thus, organoids can be grown from cryopreserved primary human adult pancreatic tissue.

Human pancreatic organoids generate insulin-producing cells *in vivo*

While the *in vitro* differentiation experiments indicated differentiation toward an endocrine lineage based on gene expression analysis, only a few INS$^+$ cells were observed. It is well known that human ESC differentiate into insulin-producing cells after implantation into mice[42]. Therefore, we tested the capacity of pancreatic organoids to further differentiate *in vivo* after transplantation under the kidney capsule of immunodeficient mice. One day after transplantation the majority of grafted cells were KRT19$^+$ and no INS$^+$ cells were observed (**Figure 5A**). However, pancreatic organoids from the same donor 1 month after transplantation showed INS$^+$ cells within the ductal lining (**Figure 5B**). Organoids derived from each donor (n = 8) were able to generate 1.5% ± 0.2% INS$^+$ cells within the ductal lining (n = 8; **Figure 5B**). No difference in the proportion of INS$^+$ cells was observed in the hyperglycemic animals (**Figure 5C**). Production of insulin was confirmed by immunostaining of C-peptide in INS$^+$ cells (CPEP) (**Figure S5A**). Furthermore, insulin was co-expressed with several functional endocrine markers (PDX1, IAPP, NKX6.1, and SYP) but not with GCG (**Figure S5B-S5E**).

The differentiation phase *in vitro* was necessary for the appearance of INS^+ cells as transplantation of organoids 1 week after expansion yielded either no grafts or only large cystic structures with no hormone-positive cells (data not shown).

Human C-peptide could be readily measured in normoglycemic and hyperglycemic mice after a glucose challenge indicating that human insulin was released into the circulation upon a common beta cell stimulus (**Figure 5D**). Basal human C-peptide was also present in normoglycemic mice before the glucose challenge (89.2 ± 59.9 pmol/L, n = 8). Blood glucose of grafted mice did not decrease significantly in either hyperglycemic mice (26.5 ± 3.9 mmol/L at day 0 versus 24.3 ± 3.8 mmol/L at day 30, n = 8) or in the normoglycemic group (8.6 ± 1.3 mmol/L at day 0 versus 6.7 ± 2.4 mmol/L at day 30, n = 8). Thus, graft function was detectable but not sufficient to restore normoglycemia within 1 month after organoid transplantation in hyperglycemic mice.

Sorted $ALDH^{hi}$ cells derived from organoids expanded for 7 days were also differentiated for 1 week *in vitro* and subsequently transplanted under the kidney capsule of normoglycemic immunodeficient mice. After 50 days, retrieved grafts contained both $KRT19^+$ and C-$peptide^+$ cells (**Figure 5E**).

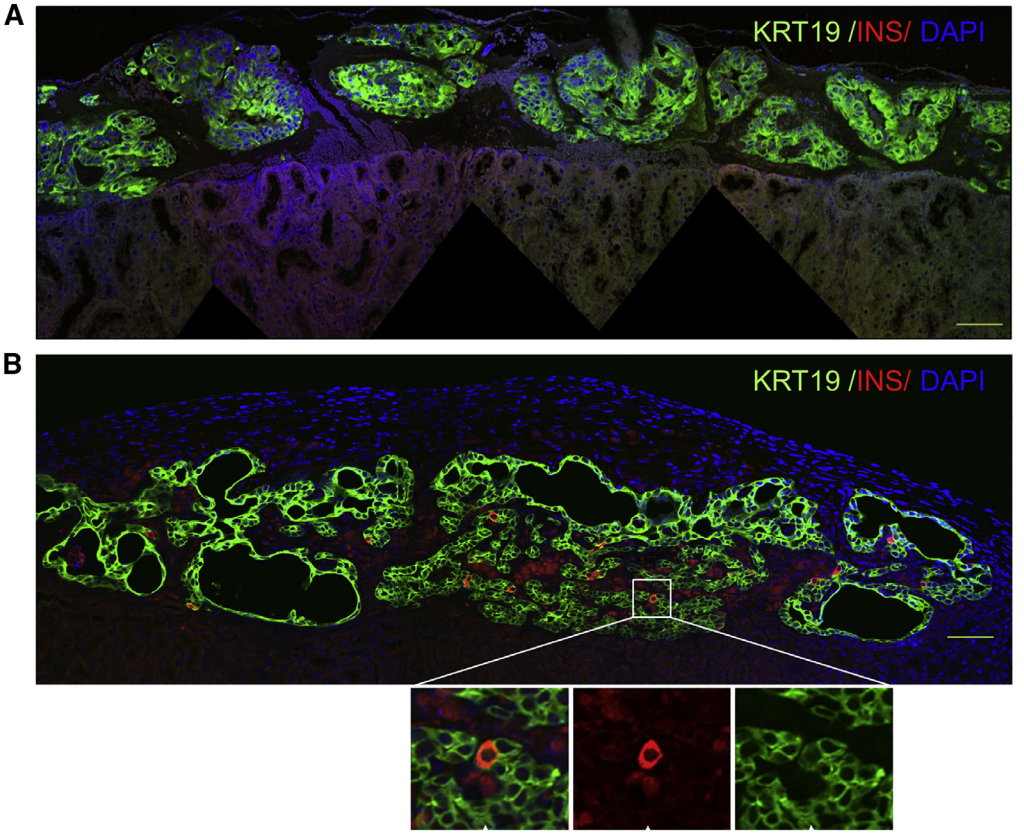
A
KRT19 /INS/ DAPI
B
KRT19 /INS/ DAPI

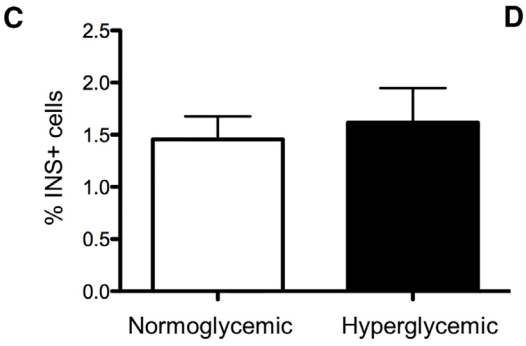
C
% INS+ cells
2.5
2.0
1.5
1.0
0.5
0.0
Normoglycemic
Hyperglycemic

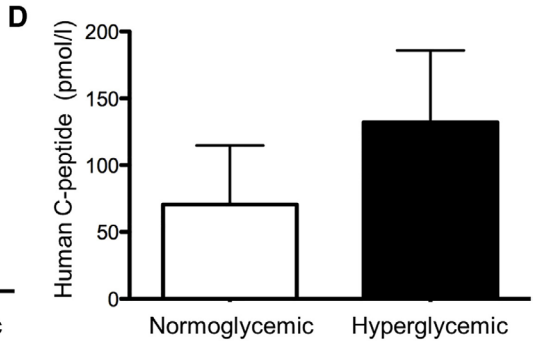
D
Human C-peptide (pmol/l)
200
150
100
50
0
Normoglycemic
Hyperglycemic

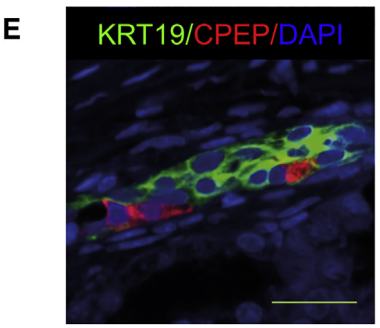
E
KRT19/CPEP/DAPI

Figure 5. Human pancreatic organoids generate insulin-producing cells *in vivo*
Grafts composed of *in vitro* differentiated organoids derived from islet-depleted exocrine pancreatic tissue were transplanted under the mouse kidney capsule after 7 days of expansion and 7 days of differentiation. (**a**) Day 1 after transplantation. Immunostaining for KRT19 (green) and INS (red). No INS^+ cells are present. DAPI (blue) was used as nuclear counterstain. Scale bar, 50 µm. (**b**) Day 30 after transplantation. Transplanted organoids formed a ductal network (KRT19, green) and many INS^+ cells (red) are present within the ductal lining (arrows indicate INS^+ cells). DAPI (blue) was used as nuclear counterstain. Scale bar, 50 µm. (**c**) Percentage of INS^+ cells in the ductal lining 1 month after transplantation. For each donor, grafts were transplanted in both normoglycemic and hyperglycemic mice, and two mice were transplanted per donor. No significant difference in the number of INS^+ cells between the two groups of mice was found. Mean ± SEM, n = 8 donors. (**d**) Human C-peptide concentration after a glucose challenge in mice 1 month after organoid transplantation. Grafts were transplanted in either normoglycemic mice or hyperglycemic mice, and two mice were transplanted per donor. No significant difference in human C-peptide concentration between the two groups of mice was observed. Mean ± SEM, n = 8 donors. (**e**) Confocal image of a graft of sorted $ALDH^{hi}$ cells isolated from organoids after expansion for 7 days. The $ALDH^{hi}$ cells were differentiated for 7 days in vitro before transplantation under the kidney capsule of normoglycemic mice (n = 3 donors, 1 mouse per donor). The graft was retrieved after 50 days and contained both $KRT19^+$ and $CPEP^+$ cells. Cells co-expressing KRT19 and C-peptide indicate a transition stage from a duct (-like) phenotype to a beta (-like) cell phenotype. DAPI (blue) was used as nuclear counterstain. Scale bar, 50 µm. See also **Figure S5**.

Discussion

Our data indicate that adult human pancreatic tissue can be expanded as 3D organoids and long-term expansion can be achieved by passaging these pancreatic organoids. Cryopreservation of the pancreatic tissue is possible without losing these characteristics. A subpopulation of cells from the organoids have progenitor characteristics and give rise to endocrine cells after transplantation.

Progress to expand human adult pancreatic tissue and thus exploration of its capacity for endocrine cell differentiation has been hampered by epithelial-to-mesenchymal transition in 2D culture systems. The 3D culture system we have developed here provides an environment that allows substantial growth of human pancreatic cells starting from minced tissue. Recently we showed that adult mouse pancreatic organoids can also be expanded using similar culture conditions[32]. We and others described Matrigel-based culture methods for expansion of dispersed exocrine cells from adult mouse[32,34] and human[43] pancreas and for expansion of genetically modified human pancreatic ductal cells[44]. The striking aspect of our expansion protocol is the self-organisation of the tissue into organoids with complex budding structures. These organoids display a remarkable $KRT19^+$ epithelial tree-like structure with apical-basal polarity. This configuration has been shown for mouse embryonic pancreas tissue *in vivo* and *in vitro*[30,36], and is present during human pancreatic organogenesis[45]. Similar culture systems enabled the expansion of human intestine and stomach in complex cell configurations, also called organoids, that appear to recapitulate organogenesis and tissue regeneration[31,46].

During embryogenesis, the tip regions of the expanding ductal trees in the developing pancreas harbor progenitor cells[21,36,45]; and, in adult human tissue, we predicted, from single-cell

transcriptome data, that the progenitor population in human adult pancreatic cells resides among the ductal population[16]. The morphology of the pancreatic organoids (derived from adult pancreatic tissue) in our study allowed us to search for putative progenitors in the budding structures. ALDH^{hi} cells had differentially high expression of the progenitor markers PDX1, CPA1, MYC, and PTF1A[36]. In addition, we established organoid culture from human fetal pancreatic tissue. These fetal pancreatic organoids also contained ALDH^{hi} cells in budding structures. Interestingly, transcriptional profiling revealed that ALDH^{hi} cells from adult pancreatic organoids were closer to ALDH^{hi} cells from fetal pancreatic organoids than to adult exocrine tissue (*i.e.*, the islet-depleted tissue before expansion). This indicates a reprogramming of a subset of adult pancreatic cells to a progenitor-like stage.

Organoids expanded from human pancreas and transplanted in immunodeficient mice gave rise to insulin-producing cells after 1 month. The location of the insulin-producing cells in the grafts, *i.e.*, in close proximity of or within the ductal lining, and the increased number of insulin-positive cells after engraftment compared with the initial cell population, support the concept that these cells were newly generated. However, while human C-peptide could be detected in the circulation the number of beta cells was not sufficient to restore normoglycemia in diabetic mice 1 month after transplantation. In a recent study by Lee et al.[44], the authors also showed that a subpopulation of expanded ductal cells could differentiate to insulin-secreting cells using an alternative approach of adenovirus-mediated expression of pro-endocrine factors and co-transplantation with mouse embryonic fibroblasts. In summary, although culture conditions need to be optimised to increase graft efficacy, our study provides a proof-of-concept that this 3D culture system can be used to expand primary human ductal cells that can differentiate to an endocrine fate without the need for genetic modification.

The origin of the ALDH^{hi} cells in our system is unclear. An ALDH^{hi} progenitor cell population has been identified in a subset of adult ductal/CAC cells[39] and in the developing pancreas[38] of mice, and these cells had the ability to self-renew and to differentiate into both endocrine and exocrine cells.

Notably, several studies have recently attributed a functional role to ALDH1 isoforms during pancreas development in humans[47], mice[48], and zebrafish[49]. Our data indicate that the specific culture conditions we developed support this progenitor state. Whether these ALDH^{hi} cells have a CAC origin or not warrants further investigation. At present this question is challenging as there is a lack of markers specific for human adult CACs. In mature murine pancreas, HES1 expression marks terminal ductal or CACs, whereas it identifies MPCs in early embryonic pancreas (until e11.5), and exocrine-restricted progenitors from e13.5 until birth[40]. Here, we found that HES1 was slightly upregulated at the mRNA level in ALDH^{hi} cells, but HES1 protein expression was not restricted to the tips of the budding structures where the majority of ALDH^{hi} cells reside. Finally, the ALDH^{hi} population is heterogeneous, with only a small proportion of cells able to expand *in vitro*. Therefore, additional cell surface markers will be necessary to efficiently enrich and characterize the progenitor subpopulation from this heterogeneous population of ALDH^{hi} cells.

It has been unclear whether an endocrine/multipotent progenitor population exists in the

adult human pancreas. Indeed, classical definitions of what constitutes an adult stem cell population are under debate[50]. However, we provide a proof-of-concept for the existence of a $ALDH^{hi}$ population of human pancreatic cells (most likely $KRT19^{+}$ cells) that appears under specific culture conditions, and that has the capacity to differentiate into an endocrine cell phenotype. Aldefluor has been used to detect $ALDH^{hi}$ stem/progenitor cells in multiple tissues[51]. Here, we show that this cell population expresses the pancreatic progenitor markers CPA1, PDX1, MYC, and PTF1A. Furthermore, the gene expression profile of adult pancreatic $ALDH^{hi}$ population presents a high degree of similarity with fetal pancreatic $ALDH^{hi}$ cells.

Finally, since these cells are derived from the adult human pancreas and, thus, have already committed to a pancreatic fate, differentiation to the beta cell lineage may be easier to achieve than differentiation of other adult stem/progenitor cells. In current allogeneic and autologous islet transplantation contaminating non-islet cells from the human pancreas are always co-transplanted with islets into human recipients without adverse effects[52]. Therefore, expanded and differentiated adult human pancreatic cells are likely to be relatively safe compared with embryonic or induced pluripotent cell lines for future beta cell replacement therapy programs.

Experimental procedures

Human primary tissue

Adult Pancreatic Tissue Islet-depleted pancreatic tissue and human islets that could not be used for clinical transplantation were used in the studies according to national laws and if research consent was available.

Fetal Pancreatic Tissue Fetal pancreatic tissue from elective abortions was used after written (parental) informed consent was provided. Collection and use of human fetal tissue for research was approved by the Medical Ethics committee of the LUMC.

Generation of human and fetal pancreatic organoids

Human adult islet-depleted pancreatic tissue was obtained after human islet isolation procedures. For culture of adult pancreatic organoids, small pieces of exocrine tissue were plated and expanded in Matrigel (BD Biosciences). Human fetal pancreatic tissue was obtained from fetuses with a gestational age of 9, 20, and 22 weeks. For culture of fetal pancreatic organoids, small pieces of human fetal pancreatic tissue were plated and expanded in Matrigel similar to adult pancreatic organoids. A progenitor population within the organoids was identified using the Aldefluor fluorescent reagent system (STEMCELL), which is based on detection of high ALDH activity in progenitor cells. $ALDH^{hi}$ and $ALDH^{lo}$ cell populations were sorted and plated in Matrigel before analysis. Human and fetal pancreatic organoids were analysed by immunohistochemistry, RNA sequencing, qPCR, and smFISH. For a detailed description, see Supplemental Experimental Procedures.

In vitro and *in vivo* differentiation of human pancreatic organoids

After expansion, adult pancreatic organoids were retrieved from the Matrigel and analysed, cryopreserved in liquid nitrogen, or transferred to a differentiation culture medium (3 mL), characterised by absence of growth factors, in six-well hydrophobic plates (Corning). Organoids were cultured for 7-18 days before analysis or transplantation under the kidney capsule in normoglycemic or hyperglycemic immunodeficient mice. Human C-peptide was measured and grafts were analysed up to 1 month after transplantation. For a detailed description, see Supplemental Experimental Procedures.

Acknowledgement

This work was financially supported by the DON foundation, the Dutch Diabetes Research Foundation, the Tjanka Foundation, and the Diabetes Cell Therapy Initiative. We thank Dr. Vrolijk for help with analyses of immunostaining (ImageJ-based data analyses), Yves Heremans (H.H. lab) and Annemieke Tons (Leiden University Medical Center, Leiden) for helping with the NEUROG3 staining, the Hubrecht imaging center for microscope assistance, and Stefan van der Elst (Geijsen lab, Hubrecht Institute, Utrecht) for help with FACS and analysis.

References

1. Nijhoff, M.F., *et al.* Glycemic Stability Through Islet-After-Kidney Transplantation Using an Alemtuzumab-Based Induction Regimen and Long-Term Triple-Maintenance Immunosuppression. *Am J Transplant* **16**, 246-253 (2016).
2. Ricordi, C., Lacy, P.E. & Scharp, D.W. Automated islet isolation from human pancreas. *Diabetes* **38 Suppl 1**, 140-142 (1989).
3. Russ, H.A., Bar, Y., Ravassard, P. & Efrat, S. In vitro proliferation of cells derived from adult human beta-cells revealed by cell-lineage tracing. *Diabetes* **57**, 1575-1583 (2008).
4. Gershengorn, M.C., *et al.* Epithelial-to-mesenchymal transition generates proliferative human islet precursor cells. *Science* **306**, 2261-2264 (2004).
5. Hrvatin, S., *et al.* Differentiated human stem cells resemble fetal, not adult, beta cells. *Proc Natl Acad Sci U S A* **111**, 3038-3043 (2014).
6. Pagliuca, F.W., *et al.* Generation of functional human pancreatic beta cells in vitro. *Cell* **159**, 428-439 (2014).
7. Rezania, A., *et al.* Reversal of diabetes with insulin-producing cells derived in vitro from human pluripotent stem cells. *Nat Biotechnol* **32**, 1121-1133 (2014).
8. Lund, R.J., Narva, E. & Lahesmaa, R. Genetic and epigenetic stability of human pluripotent stem cells. *Nat Rev Genet* **13**, 732-744 (2012).
9. Mummery, C. Induced pluripotent stem cells--a cautionary note. *N Engl J Med* **364**, 2160-2162 (2011).
10. Butler, A.E., *et al.* Beta-cell deficit and increased beta-cell apoptosis in humans with type 2 diabetes. *Diabetes* **52**, 102-110 (2003).
11. Butler, A.E., *et al.* Adaptive changes in pancreatic beta cell fractional area and beta cell turnover in human pregnancy. *Diabetologia* **53**, 2167-2176 (2010).
12. Bonner-Weir, S., *et al. In vitro* cultivation of human islets from expanded ductal tissue. *Proc Natl Acad Sci U S A* **97**, 7999-8004 (2000).
13. Yatoh, S., *et al.* Differentiation of affinity-purified human pancreatic duct cells to beta-cells. *Diabetes* **56**, 1802-1809 (2007).
14. Lee, J.H., Jo, J., Hardikar, A.A., Periwal, V. & Rane, S.G. Cdk4 regulates recruitment of quiescent beta-cells and ductal epithelial progenitors to reconstitute beta-cell mass. *PLoS One* **5**, e8653 (2010).
15. Klein, D., *et al.* BMP-7 Induces Adult Human Pancreatic Exocrine-to-Endocrine Conversion. *Diabetes* **64**, 4123-4134 (2015).
16. Grun, D., *et al.* De Novo Prediction of Stem Cell Identity using Single-Cell Transcriptome Data. *Cell Stem Cell* **19**, 266-277 (2016).
17. Inada, A., *et al.* Carbonic anhydrase II-positive pancreatic cells are progenitors for both endocrine and exocrine pancreas after birth. *Proc Natl Acad Sci U S A* **105**, 19915-19919 (2008).
18. Xu, X., *et al.* Beta cells can be generated from endogenous progenitors in injured adult mouse pancreas. *Cell* **132**, 197-207 (2008).
19. Criscimanna, A., *et al.* Duct cells contribute to regeneration of endocrine and acinar cells following pancreatic damage in adult mice. *Gastroenterology* **141**, 1451-1462, 1462 e1451-1456 (2011).
20. Al-Hasani, K., *et al.* Adult duct-lining cells can reprogram into beta-like cells able to counter repeated cycles of toxin-induced diabetes. *Dev Cell* **26**, 86-100 (2013).
21. Solar, M., *et al.* Pancreatic exocrine duct cells give rise to insulin-producing beta cells during embryogenesis but not after birth. *Dev Cell* **17**, 849-860 (2009).
22. Kopp, J.L., *et al.* Sox9$^+$ ductal cells are multipotent progenitors throughout development but do not produce new endocrine cells in the normal or injured adult pancreas. *Development* **138**, 653-665 (2011).
23. Furuyama, K., *et al.* Continuous cell supply from a Sox9-expressing progenitor zone in adult liver, exocrine pancreas and intestine. *Nat Genet* **43**, 34-41 (2011).
24. Russ, H.A., Ravassard, P., Kerr-Conte, J., Pattou, F. & Efrat, S. Epithelial-mesenchymal transition in cells expanded in vitro from lineage-traced adult human pancreatic beta cells. *PLoS One* **4**, e6417 (2009).
25. Gao, R., *et al.* Characterization of endocrine progenitor cells and critical factors for their differentiation in human adult pancreatic cell culture. *Diabetes* **52**, 2007-2015 (2003).
26. Seeberger, K.L., *et al.* Expansion of mesenchymal stem cells from human pancreatic ductal epithelium. *Lab Invest* **86**, 141-153 (2006).
27. Todorov, I., *et al.* Generation of human islets through expansion and differentiation of non-islet pancreatic cells discarded (pancreatic discard) after islet isolation. *Pancreas* **32**, 130-138 (2006).
28. Kesavan, G., *et al.* Cdc42-mediated tubulogenesis controls cell specification. *Cell* **139**, 791-801 (2009).
29. Cortijo, C., Gouzi, M., Tissir, F. & Grapin-Botton, A. Planar cell polarity controls pancreatic beta cell differentiation and glucose homeostasis. *Cell Rep* **2**, 1593-1606 (2012).
30. Greggio, C., *et al.* Artificial three-dimensional niches deconstruct pancreas development *in vitro*. *Development* **140**, 4452-4462 (2013).
31. Sato, T., *et al.* Long-term expansion of epithelial organoids from human colon, adenoma, adenocarcinoma, and Barrett's epithelium. *Gastroenterology* **141**, 1762-1772 (2011).
32. Huch, M., *et al.* Unlimited in vitro expansion of adult bi-potent pancreas progenitors through the Lgr5/R-spondin axis. *EMBO J* **32**, 2708-2721 (2013).
33. Huch, M., *et al.* In vitro expansion of single Lgr5$^+$ liver stem cells induced by Wnt-driven regeneration. *Nature* **494**, 247-250 (2013).
34. Jin, L., *et al.* Colony-forming cells in the adult mouse pancreas are expandable in Matrigel and form endocrine/acinar colonies in laminin hydrogel. *Proc Natl Acad Sci U S A* **110**, 3907-3912 (2013).
35. Ouziel-Yahalom, L., *et al.* Expansion and redifferentiation of adult human pancreatic islet cells. *Biochem Biophys Res Commun* **341**, 291-298 (2006).
36. Zhou, Q., Brown, J., Kanarek, A., Rajagopal, J. & Melton, D.A. In vivo reprogramming of adult pancreatic exocrine cells to beta-cells. *Nature* **455**, 627-632 (2008).
37. Shih, H.P., Wang, A. & Sander, M. Pancreas organogenesis: from lineage determination to morphogenesis. *Annu Rev Cell Dev Biol* **29**, 81-105 (2013).
38. Ioannou, M., *et al.* ALDH1B1 is a potential stem/progenitor marker for multiple pancreas progenitor pools. *Dev Biol* **374**, 153-163 (2013).
39. Rovira, M., *et al.* Isolation and characterization of centroacinar/terminal ductal progenitor cells in adult mouse pancreas. *Proc Natl Acad Sci U S A* **107**, 75-80 (2010).
40. Kopinke, D. & Murtaugh, L.C. Exocrine-to-endocrine differentiation is detectable only prior to birth in the uninjured mouse pancreas. *BMC Dev Biol* **10**, 38 (2010).
41. Gao, R., Ustinov, J., Korsgren, O. & Otonkoski, T. In vitro neogenesis of human islets reflects the plasticity

of differentiated human pancreatic cells. *Diabetologia* **48**, 2296-2304 (2005).
42. Kroon, E.*, et al.* Pancreatic endoderm derived from human embryonic stem cells generates glucose-responsive insulin-secreting cells in vivo. *Nat Biotechnol* **26**, 443-452 (2008).
43. Boj, S.F.*, et al.* Organoid models of human and mouse ductal pancreatic cancer. *Cell* **160**, 324-338 (2015).
44. Lee, J.*, et al.* Expansion and conversion of human pancreatic ductal cells into insulin-secreting endocrine cells. *Elife* **2**, e00940 (2013).
45. Jennings, R.E.*, et al.* Development of the human pancreas from foregut to endocrine commitment. *Diabetes* **62**, 3514-3522 (2013).
46. Barker, N.*, et al.* Lgr5($^+$ve) stem cells drive self-renewal in the stomach and build long-lived gastric units in vitro. *Cell Stem Cell* **6**, 25-36 (2010).
47. Li, J.*, et al.* Aldehyde dehydrogenase 1 activity in the developing human pancreas modulates retinoic acid signaling in mediating islet differentiation and survival. *Diabetologia* **57**, 754-764 (2014).
48. Ostrom, M.*, et al.* Retinoic acid promotes the generation of pancreatic endocrine progenitor cells and their further differentiation into beta-cells. *PLoS One* **3**, e2841 (2008).
49. Matsuda, H., Parsons, M.J. & Leach, S.D. Aldh1-expressing endocrine progenitor cells regulate secondary islet formation in larval zebrafish pancreas. *PLoS One* **8**, e74350 (2013).
50. Clevers, H. STEM CELLS. What is an adult stem cell? *Science* **350**, 1319-1320 (2015).
51. Balber, A.E. Concise review: aldehyde dehydrogenase bright stem and progenitor cell populations from normal tissues: characteristics, activities, and emerging uses in regenerative medicine. *Stem Cells* **29**, 570-575 (2011).
52. Ichii, H.*, et al.* Characterization of pancreatic ductal cells in human islet preparations. *Lab Invest* **88**, 1167-1177 (2008).

Supplemental information